Genome-Wide Comparison of Medieval and Modern *Mycobacterium leprae*

Verena J. Schuenemann *et al.*

Science **341**, 179 (2013);
DOI: 10.1126/science.1238286

functionally examined genes that were tightly coexpressed and positioned elsewhere in the genome that belong to the CYP72 subfamily of cytochrome P450s (i.e., GAME7 and GAME8). GAME7 was coexpressed in both species, whereas StGAME8a and StGAME8b were strongly coexpressed with *StSGT1* and *StGAME4* in potato. At present, we could not demonstrate SGA-related activity for GAME7, although as for GAME6, it was suggested to be involved in SGA metabolism (*12*). Yet, *GAME8*-silenced tomato leaves accumulated 22-(*R*)-hydroxycholesterol (fig. S6, N to Q), a proposed intermediate in the SGA biosynthetic pathway (Fig. 1).

The above findings allowed us to propose a pathway from cholesterol to α-tomatine. Cholesterol is hydroxylated at C22 by GAME7 (*12*), followed by GAME8 hydroxylation at the C26 position (Fig. 1). The 22,26-dihydroxycholesterol is then hydroxylated at C16 and oxidized at C22, followed by closure of the *E*-ring by GAME11 and GAME6 to form the furostanol-type aglycone. This order of reactions is supported by the accumulation of cholestanol-type saponins, lacking hydroxylation at C16 and the hemi-acetal *E*-ring when silencing *GAME11* (fig. S6, F to I). The furostanol-intermediate is oxidized by GAME4 to its 26-aldehyde, which is the substrate for transamination catalyzed by GAME12. Nucleophilic attack of the amino nitrogen at C22 leads to the formation of tomatidenol, which is dehydrogenated to tomatidine. Tomatidine is subsequently converted by GAME1 to T-Gal (*9*). T-Gal in its turn is glucosylated by GAME17 into γ-tomatine, which is further glucosylated by GAME18 to β1-tomatine that is finally converted to α-tomatine by GAME2 (Fig. 1).

Some specialized plant metabolites, particularly terpenoids, are the result of activities from clusters of genes (*15*, *16*). The existence of metabolic gene clusters raises questions about the advantages of such genomic organization (*17*). Reducing the distance between loci, resulting in coinheritance of advantageous combinations of alleles, may be one benefit of clustering (*17*). Clustering glycosyltransferases and core pathway genes, as observed here for SGAs, could maintain allelic combinations that support the metabolic outcome needed by the plant and reduce formation of phytotoxic aglycone compounds (*9*, *18*). We found that the regions of coexpressed genes in both chromosomes (i.e., 7 and 12) were flanked by similarly annotated genes and positioned identically along the genome, although poorly coexpressed with *GAME1*/*SGT1* and *GAME4* and likely not related to SGA metabolism (fig. S11 and table S13). This suggests a duplication event that facilitated the positioning alongside each other on chromosome 12 of *GAME4* and *GAME12*, both STSs and SGAs branch-point genes. Subsequent evolution of enzyme function of this gene pair likely allowed plants in the *Solanaceae* family to start producing the nitrogen-containing steroidal alkaloids.

We have shown that SGA levels can be severely reduced in potato tubers by modifying expression of an enzyme in the biosynthetic pathway. The lack of SGAs in such plants might make them sensitive to biotic stress, and the increased production of STSs (as occurred in *GAME4*-silenced plants)—which are nontoxic to warm-blooded species, including humans (*19*)—might provide a compensatory defense mechanism (*20*). The findings open the way for developing new strategies, through genetic engineering or more classical breeding programs, to reduce quantities of the antinutritional SGAs in key crops of the *Solanaceae*, including potato, tomato, and eggplant. At the same time, it provides a platform for studying the SGA and STS biosynthetic pathways, transport, and regulatory systems that control the production of thousands of these chemicals in specific plant lineages.

References and Notes

1. N. N. Narayanan, U. Ihemere, C. Ellery, R. T. Sayre, *PLoS ONE* **6**, e21996 (2011).
2. L. C. Dolan, R. A. Matulka, G. A. Burdock, *Toxins* **2**, 2289–2332 (2010).
3. L. L. Sanford, S. P. Kowalski, C. M. Ronning, K. L. Deahl, *Am. J. Potato Res.* **75**, 167–172 (1998).
4. M. Friedman, *J. Agric. Food Chem.* **54**, 8655–8681 (2006).
5. M. Desfosses, *J. Pharmacie* **6**, 374–376 (1820).
6. J. G. Roddick, *Phytochemistry* **28**, 2631–2634 (1989).
7. FDA Poisonous Plant Database, www.accessdata.fda.gov/scripts/Plantox/
8. K. F. McCue *et al.*, *Plant Sci.* **168**, 267–273 (2005).
9. M. Itkin *et al.*, *Plant Cell* **23**, 4507–4525 (2011).
10. E. Eich, *Solanaceae and Convolvulaceae: Secondary Metabolites: Biosynthesis, Chemotaxonomy, Biological and Economic Significance* (Springer, Berlin, 2008).
11. The Potato Genome Sequencing Consortium, *Nature* **475**, 189–195 (2011).
12. N. Umemoto, S. Katsunori, U.S. Patent application 20120159676 A1 (2012).
13. T. Yamanaka *et al.*, *J. Agric. Food Chem.* **57**, 3786–3791 (2009).
14. Materials and methods are available as supplementary materials on *Science* Online.
15. D. J. Kliebenstein, A. Osbourn, *Curr. Opin. Plant Biol.* **15**, 415–423 (2012).
16. T. Winzer *et al.*, *Science* **336**, 1704–1708 (2012).
17. A. E. Osbourn, *Plant Physiol.* **154**, 531–535 (2010).
18. B. Field, A. E. Osbourn, *Science* **320**, 543–547 (2008).
19. P. F. Dowd, M. A. Berhow, E. T. Johnson, *J. Chem. Ecol.* **37**, 443–449 (2011).
20. S. G. Sparg, M. E. Light, J. van Staden, *J. Ethnopharmacol.* **94**, 219–243 (2004).

Acknowledgments: We thank A. Tishbee and R. Kramer for operating the UPLC-qTOF-MS instrument and the European Research Council (SAMIT-FP7 program) for supporting the work in the A.A. laboratory. A.A. is the incumbent of the Peter J. Cohn Professorial Chair. J.B. was supported by the European Union 7th Frame Anthocyanin and Polyphenol Bioactives for Health Enhancement through Nutritional Advancement (ATHENA) Project (FP7-KBBE-2009-3-245121-ATHENA). U.H. was partially supported by fellowship AZ: I/82 754, Volkswagen Foundation, Hannover, Germany. We thank the Council of Scientific and Industrial Research (India) for support to A.P.G. (Raman Research Fellowship), A.J.B., Y.C., and P.S. (Research Fellowship) and the University Grants Commission (India) for supporting B.S. We also thank D. R. Nelson for assistance with CYP450 gene classification and R. Last for critically reading the manuscript. A.A. and M.I. are inventors on publication number WO2012095843 A1, submitted by Yeda Research and Development Co. Ltd, which covers the use of the *GAME4* gene for generating low-alkaloid fruit and tubers.

Supplementary Materials

www.sciencemag.org/cgi/content/full/science.1240230/DC1
Materials and Methods
Figs. S1 to S15
Tables S1 to S16
References (*21*–*31*)

8 May 2013; accepted 6 June 2013
Published online 20 June 2013;
10.1126/science.1240230

Genome-Wide Comparison of Medieval and Modern *Mycobacterium leprae*

Verena J. Schuenemann,[1]* Pushpendra Singh,[2]* Thomas A. Mendum,[3]* Ben Krause-Kyora,[4]* Günter Jäger,[5]* Kirsten I. Bos,[1] Alexander Herbig,[5] Christos Economou,[6] Andrej Benjak,[2] Philippe Busso,[2] Almut Nebel,[4] Jesper L. Boldsen,[7] Anna Kjellström,[8] Huihai Wu,[3] Graham R. Stewart,[3] G. Michael Taylor,[3] Peter Bauer,[9] Oona Y.-C. Lee,[10] Houdini H.T. Wu,[10] David E. Minnikin,[10] Gurdyal S. Besra,[10] Katie Tucker,[11] Simon Roffey,[11] Samba O. Sow,[12] Stewart T. Cole,[2]† Kay Nieselt,[5]† Johannes Krause[1]†

Leprosy was endemic in Europe until the Middle Ages. Using DNA array capture, we have obtained genome sequences of *Mycobacterium leprae* from skeletons of five medieval leprosy cases from the United Kingdom, Sweden, and Denmark. In one case, the DNA was so well preserved that full de novo assembly of the ancient bacterial genome could be achieved through shotgun sequencing alone. The ancient *M. leprae* sequences were compared with those of 11 modern strains, representing diverse genotypes and geographic origins. The comparisons revealed remarkable genomic conservation during the past 1000 years, a European origin for leprosy in the Americas, and the presence of an *M. leprae* genotype in medieval Europe now commonly associated with the Middle East. The exceptional preservation of *M. leprae* biomarkers, both DNA and mycolic acids, in ancient skeletons has major implications for palaeomicrobiology and human pathogen evolution.

Leprosy, which results from infection with the unculturable pathogen *Mycobacterium leprae*, was common in Europe until the 16th century, when it essentially disappeared. In contrast, disease prevalence has remained high in the developing world. During the past 20 years,

elimination efforts using multidrug therapy have been largely successful, leading to the perception that leprosy is no longer a global health threat despite an annual incidence of over 225,000 cases worldwide (*1*). To understand the evolution and phylogeography of the leprosy bacillus and to investigate the disappearance of leprosy from Europe, we have used DNA capture techniques and high-throughput sequencing (HTS) to obtain near-complete genome sequences of *M. leprae* from 11th- to 14th-century skeletal remains and from recent biopsies of leprosy patients.

The 3.3 Mb genome of *M. leprae* has undergone massive gene decay (*2*), and half of the coding potential has been lost, as reflected by the presence of ~1300 pseudogenes. This reductive evolution offers an explanation for the long generation time—~14 days in humans—and our inability to culture the bacillus in vitro (*2*). The phylogeny of modern *M. leprae* has been investigated by using genome sequencing and a combination of variable number tandem repeat and single-nucleotide polymorphism (SNP) typing, defining four major branches (*3*–*5*). However, very little is known about the strains responsible for leprosy in the past. Leprosy is among the few infections that contribute to skeletal changes; hence, attempts to trace its course through history have been made in an archaeological context (*6*). Molecular biomarkers have permitted detection of *M. leprae* in skeletal remains from many different time periods and geographical locations (*7*, *8*). Studying ancient DNA (aDNA) by using a capture approach has the potential to provide new insight into pathogen evolution, as recently illustrated through full-genome reconstruction of *Yersinia pestis* from skeletal remains (*9*).

Extracts of bone and teeth from 22 medieval skeletons (Fig. 1, table S1, and supplementary materials notes 1 and 2) with osteological lesions suggestive of leprosy—from cemeteries in Denmark (n = 8 extracts) (*10*), Sweden (n = 8 extracts) (*7*), and the United Kingdom (n = 6 extracts) (*11*)—were screened for the presence of *M. leprae* DNA by using a bead capture approach of three genomic loci (*12*). Human mitochondrial DNA (mtDNA) fragments were enriched simultaneously in order to evaluate the characteristic nucleotide misincorporation patterns expected of ancient human (*13*) and pathogen DNA (*14*) so as to confirm their authentic ancient origin (supplementary materials note 3). Although DNA damage patterns corresponding to a medieval origin were found in the human mtDNA (*15*), the captured *M. leprae* DNA revealed much less damage (tables S1 and S2 and figs. S1 to S3), an observation that was entirely unexpected. We therefore relied on traditional authenticity criteria including blank controls, independent replication (*16*), and other biomarkers, such as mycolic acids (supplementary materials notes 4, 6, and 10; figs. S4 and S5; and tables S4 to S7). Five skeletal samples (3077 from Sweden, Jorgen_625 and Refshale_16 from Denmark, and SK8 and SK14 from the United Kingdom) (table S2) fulfilled our initial criterion for progression to HTS, performed before and after DNA repair (supplementary materials notes 2 and 3). Four samples (3077, Refshale_16, SK8, and SK14) yielded insufficient DNA (table S8) and hence were enriched for *M. leprae* by using DNA array capture (supplementary materials note 5). Unexpectedly, no enrichment for Jorgen_625 was necessary because an astonishing 40% of the reads mapped to *M. leprae* (table S8). It was thus possible to do a de novo assembly providing over 100-fold genomic coverage (table S9) and 169 contigs, separated by gaps corresponding to repetitive regions (Fig. 2A), that aligned perfectly with the modern *M. leprae* reference genome (supplementary materials note 6) (*2*). De novo assembly avoids ascertainment biases in gene order that may result from mapping assemblies, although it is often unsuccessful in aDNA investigations owing to inadequate preservation. Few, if any, large insertions or deletions (InDels) have occurred during the ~1000 years that separate the ancient and modern *M. leprae* strains.

To assess the high representation of *M. leprae* sequences in Jorgen_625, the ratios were determined of *M. leprae* versus human sequences in libraries of 230 to 400 base pairs (bp) and 309 to 622 bp fragments (supplementary materials note 5) and found to be 3.3 and 9, respectively (supplementary materials note 6 and fig. S6), thus indicating less fragmentation of the *M. leprae* DNA. The fundamental structural difference between mycobacterial and eukaryotic cells likely accounts for better DNA preservation. Mycobacteria are surrounded by a robust, hydrophobic layer of

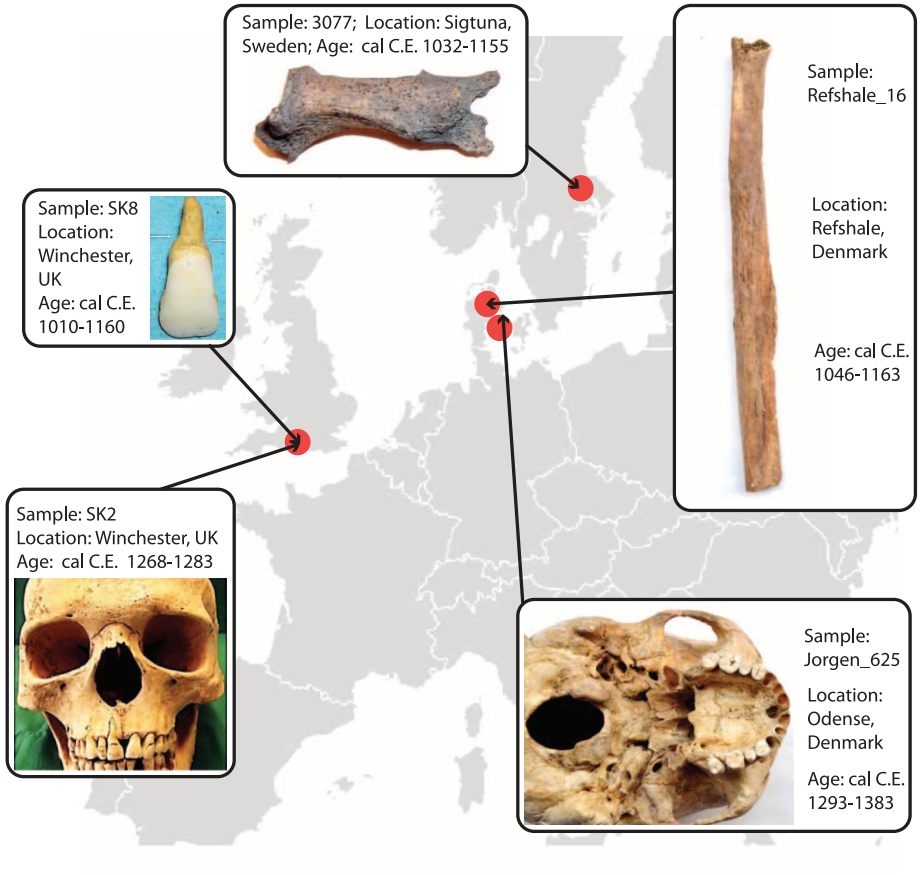

Fig. 1. Sources and origins of the five medieval *M. leprae* strains from Denmark, Sweden, and the United Kingdom for which whole-genome sequences were determined in this study. Pictures of the bones or teeth and their radiocarbon dates are shown.

[1]Institute for Archaeological Sciences, University of Tübingen, 72070 Tübingen, Germany. [2]Global Health Institute, Ecole Polytechnique Fédérale de Lausanne, 1015 Lausanne, Switzerland. [3]Department of Microbial and Cellular Sciences, Faculty of Health and Medical Sciences, University of Surrey, Guildford, GU2 7XH Surrey, UK. [4]Institute of Clinical Molecular Biology, Kiel University, 24105 Kiel, Germany. [5]Center for Bioinformatics, University of Tübingen, 72076 Tübingen, Germany. [6]Archaeological Research Laboratory, Stockholm University, SE-106 91 Stockholm, Sweden. [7]Institute of Forensic, Antropologisk Afdelin, Medicine University of Southern Denmark, 5260 Odense S, Denmark. [8]Osteoarchaeological Research Laboratory, Department of Archaeology and Classical Studies, Stockholm University, SE-106 91 Stockholm, Sweden. [9]Institute for Medical Genetics and Applied Genomics, University of Tübingen, 72076 Tübingen, Germany. [10]School of Biosciences, University of Birmingham, Edgbaston, B15 2TU Birmingham, UK. [11]Department of Archaeology, University of Winchester, Sparkford Road, SO22 4NR Winchester, UK. [12]Center for Vaccine Development-Mali, Ministry of Health, Centre National d'Appui à la lutte contre la Maladie–ex-Institut Marchoux, BP 251 Bamako, Mali.

*These authors contributed equally to this work.
†Corresponding author. E-mail: johannes.krause@uni-tuebingen.de (J.K.); kay.nieselt@uni-tuebingen.de (K.N.); stewart.cole@epfl.ch (S.T.C.)

mycolic acids that constitute more than 40% of the cell biomass (*17*). Exceptionally high amounts of mycolic acids that typify *M. leprae* were found in the tooth pulp from Jorgen_625 and, to a lesser extent, in those from SK2, SK8, SK14 (supplementary materials note 10), and Refshale_16 (fig. S5) (*11*). This finding implies that the lipid-rich cell wall protects mycobacterial DNA (*18*, *19*) from hydrolytic damage (*20*), hence the longer fragment lengths and reduced nucleotide misincorporation patterns detected.

We extended the array-based enrichment and HTS to ancient leprosy specimens (supplementary materials note 5) from Winchester in the United Kingdom (SK2 and SK14) and, as a negative control, a matched skeleton (SK12) from the same cemetery with no osteological evidence of disease. All samples from skeletons with leprosy-associated lesions (SK2, SK8, and SK14) yielded high-quality *M. leprae* reads from distinct strains. In contrast, <1% of sequences from SK12 mapped to the *M. leprae* genome, mostly to conserved regions present in all mycobacteria (table S10). This analysis further confirmed the authenticity of our samples and eliminated the possibility of cross-contamination among skeletal remains.

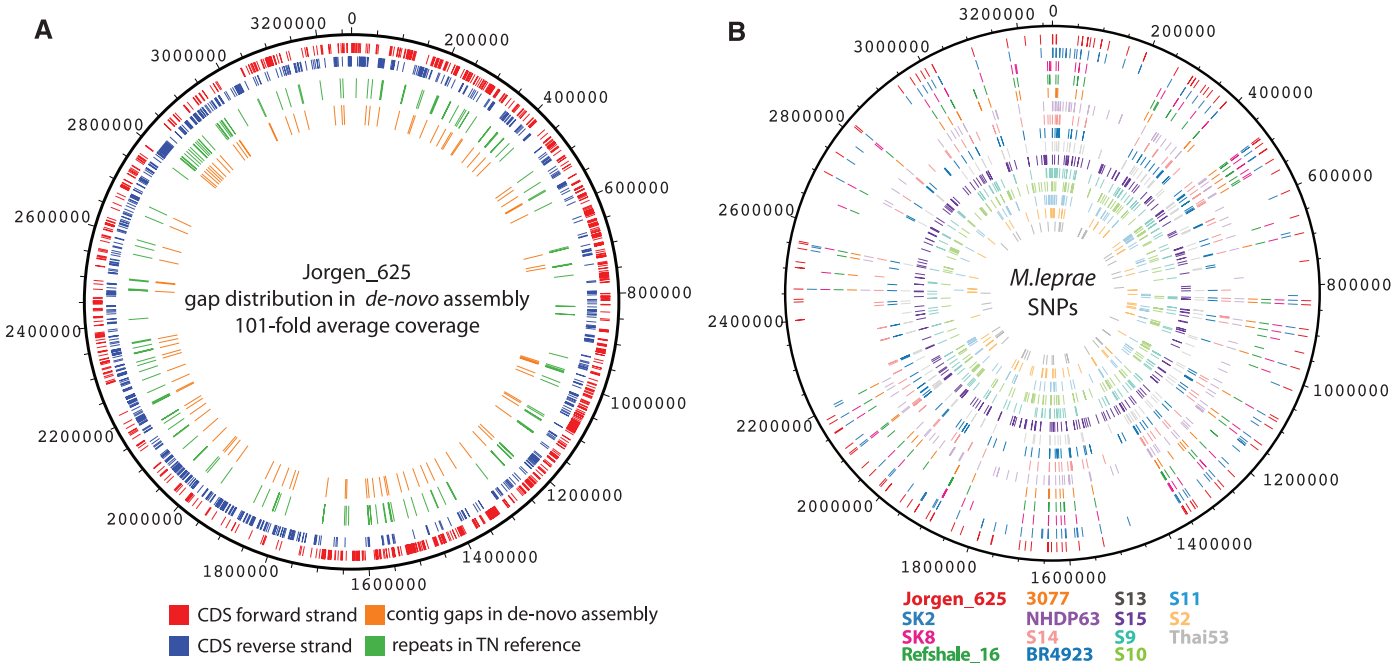

Fig. 2. De novo assembly of the ancient strain of *M. leprae* from skeleton Jorgen_625 and distribution of SNPs across all *M. leprae* genomes sequenced in this study. (**A**) All the gaps between contigs are in repetitive regions that represent ~2% of the genome of the reference strain TN. There are no structural variations and no changes in synteny, and all the coding sequences in the forward (red) and reverse (blue) strands were as in the reference genome (metagenomic analysis is available in fig. S9). (**B**) The 755 SNPs observed among the 16 genomes of *M. leprae* are represented on the 3.27-Mb circular chromosome of the TN genome. The five ancient strains sequenced in this study are shown in the outermost circles followed by 10 modern strains, colored as indicated in the key. Figures were produced with DNAPlotter (*29*).

Table 1. Ancient and modern strains of *M. leprae* whose genomes were sequenced and compared in this study, together with the reference genomes. BP, before present (in years); Ref, Reference genomes (*5*).

Sample	Serial number	Name	Radiocarbon date/year of isolation	Percent of genome reconstructed	Average fold coverage	Branch	SNP subtype	Geographic origin
Ancient	3077	3077	938 ± 19 BP	83.77%	10.13	2	2F	Sweden
	JK325	Jorgen_625	644 ± 23 BP	98.26%	101.2	3	3I	Denmark
	JK329	Refshale_16	909 ± 24 BP	97.48%	105.1	2	2F	Denmark
	SK2	SK2	729 ± 23 BP	92.88%	14.87	3	3I	UK
	SK8	SK8	1023 ± 80 BP	96.41%	20.01	2	2F	UK
Modern	S2	95034	1995	84.38%	10.25	1	1B	Antilles
	S9	96008	1996	94.51%	14.45	0	3K	New Caledonia
	S10	Ch-04	2006	96.09%	17.03	0	3K	China
	S11*	Inde 2	1990	97.59%	161.7	1	1D	India
	S13	Ml-3-28	2012	93.2%	15.12	4	4N	Mali
	S14	Ml-2-7	2012	90.53%	22.4	4	4O	Mali
	S15	92041	1992	91.73%	11.86	4 or 0	3L	New Caledonia
Ref*	TN	TN	1990			1	1A	India
	Thai53	Thai53	1982			1	1A	Thailand
	NHDP63	NHDP63	1996			3	3I	United States
	Br4923	Br4923	1996			4	4P	Brazil

*Passaged in armadillos.

A total of five medieval strains—namely 3077, Jorgen_625, Refshale_16, SK2, and SK8—satisfied our criteria for genome-wide comparison (>80% genome coverage, at least fivefold depth), enabling us to compare the genotypes of *M. leprae* strains from 11th- to 14th-century Europe with those of modern strains from different leprosy-endemic regions. For the comparison, the four available reference genome sequences (TN from India, Thai53 from Thailand, NHDP63 from the United States, and Br4923 from Brazil) (*5*) were supplemented with those of seven modern strains, each belonging to a specific SNP type or of a different geographic origin (Table 1 and table S11), obtained by using multiplexed array capture of DNA prepared directly from skin biopsies of leprosy patients or, in one case, following passage in an armadillo. Here, genome coverage ranged from 83 to 98% at 10- to 160-fold depth (Table 1 and table S9).

Whole-genome reconstructions disclosed a remarkable level of conservation (supplementary materials notes 6 and 9). In total, only 755 SNP and 57 InDels (<7 bp) were found among the 16 *M. leprae* genomes (Fig. 2B and tables S12 to S14). The distribution of the specific SNPs across all 16 genomes revealed 122, 50, and 43 distinct SNPs in modern strains S15, S10, and S9, respectively, accounting for 40% of all the genetic diversity in *M. leprae* known to date. Strains S9 and S15 harbor the $Thr^{53}Ile$ mutation in their *folP1* gene that confers dapsone-resistance (*21*). No new pseudogenes were found in ancient *M. leprae*, but five were discovered in the modern genomes. These all affect genes for conserved proteins (ML1270, ML1340, ML1761, ML0141, and ML0659) of unknown function. By far the most polymorphic gene, with a total of 11 SNPs (10 of which are nonsynonymous), is ML0411, which encodes an immunodominant serine-rich cell surface antigen (*2*), and this may reflect pressure from the host immune system.

The phylogenetic relatedness of all 16 genomes was assessed with outgroup analysis by using maximum parsimony, maximum likelihood, neighbor-joining, and Bayesian phylogeny inference (Fig. 3 and fig. S7). Most strains clustered into four major branches—which is consistent with the SNP typing scheme (*5*)—except for S9 and S10, which form the deepest lineages, and a new branch, named branch 0 (Table 1). Strain S15 also displayed deep divergence and could not be unambiguously placed among the five branches (Fig. 3). These three strains (S9, S10, and S15) were found to branch off closest to the common ancestor of *M. leprae*, *M. tuberculosis*, *M. ulcerans*, and *M. avium* (supplementary materials note 7 and figs. S7 and S8).

Two new phylogeographic conclusions can be drawn from our reconstructed *M. leprae* phylogeny. First, three ancient strains (3077, Refshale_16, and SK8) belonging to branch 2 form a tight cluster with very short branch lengths (Fig. 3A). Modern branch 2 strains have previously been reported only in Iran and Turkey (*5*), pointing to a possible link between Middle-Eastern and medieval European strains. Second, branch 3 strains have not been found in the Middle East (*5*), whereas this genotype has been detected in European skeletons (*5*, *7*, *8*), including SK2. The striking closeness of Jorgen_625 and SK2 (Fig. 3A) with the NHDP63 strain, and 52 other branch 3 strains from the United States (*22*), is consistent with the European origin of leprosy in the Americas (*4*).

Branch shortening (supplementary materials note 8) is commonly observed when ancient sequences are included in tree reconstructions owing to their lower number of derived positions. The five ancient *M. leprae* strains do indeed have shorter branch lengths than those of modern strains, which have accumulated more substitutions. The average distance of the ancient strains to the most recent common ancestor (MRCA) was 19.8 nucleotides, whereas it was 27.5 nucleotides for the modern strains, a statistically significant difference (Mann-Whitney *U* test: $U = 7.50$, $P < 0.05$).

Divergence times for the *M. leprae* strains were estimated by using the Bayesian inference software BEAST (*23*), with models of both a strict and a relaxed clock in order to compensate for possible rate variation among lineages observed in other bacterial pathogens (*24*). For both models, radiocarbon dates for ancient skeletal samples and isolation dates for the modern bacteria were used as tip calibration (supplementary materials note 8). Using the relaxed clock and 16 *M. leprae* genomes, we estimated a rate of 8.6×10^{-9} substitutions per site per year [1.32×10^{-8} to 3.61×10^{-9} 95% highest posterior density (HPD)]. Exclusion of S15 permitted the use of a strict clock, yielding an estimated rate of 6.13×10^{-9} substitutions per site per year (8.56×10^{-9} to 3.38×10^{-9} 95% HPD). The calculated mutation rate of *M. leprae* by use of direct fossil calibration is thus close to that of the related human pathogen *M. tuberculosis* by use of tip calibrations from modern strains [5.4×10^{-9} substitutions per site per year (*24*)]. It remains to be seen whether long-time fossil calibration as applied here to *M. leprae* will produce similar results for *M. tuberculosis*. The resulting divergence

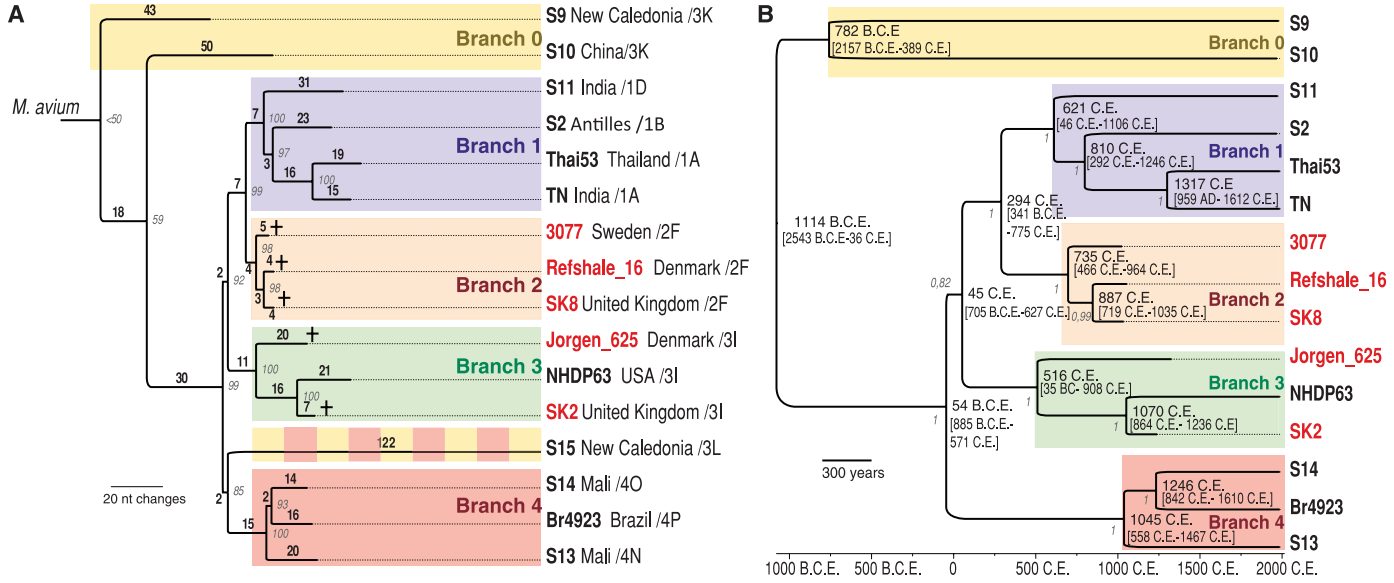

Fig. 3. Phylogeny of medieval and modern *M. leprae*. (**A**) Phylogenetic relationship of *M. leprae* genomes using a maximum parsimony tree, including *M. avium* as an outgroup. Geographic origin and SNP type are given at each branch tip. Bootstrap node support is shown in gray, and nucleotide substitutions on each branch is in bold. (**B**) Bayesian phylogenetic tree calculated with BEAST 1.7.1 (*23*), including all ancient strains with radiocarbon dates, inferred from a total of 516 genome-wide variable positions. Divergence time intervals are shown on each node in years B.C.E. and C.E. Posterior probabilities for each node are shown in gray. Labeling colors vary from red to blue based on the tip age for each branch.

times for the MRCA for all the *M. leprae* strains are 2871 years ago (1350 to 5078 years ago) and 3126 years ago (1975 to 4562 years ago) for the relaxed and strict clock models, respectively (Fig. 3B). This is consistent with the oldest known and accepted osteological evidence for leprosy from 2000 BCE. India (*25*).

The sudden decline of leprosy in 16th-century Europe was almost certainly not due to the medieval European strain of *M. leprae* losing virulence, as evidenced by the close similarity between the modern NHDP63 strain and ancient Jorgen_625 and SK2 strains. Extraneous factors—for example, other infectious diseases such as plague or tuberculosis, changes in host immunity (*26*, *27*), or improved social conditions—may have accounted for its decline. Our finding of well-preserved mycolic acids in a 14th-century tooth together with sufficient DNA to generate a whole de novo genome sequence may enable investigation of ancient leprosy bacilli and other pathogens well beyond the inferred maximum age for mammalian DNA of around 1 million years (*28*). There is thus a real prospect that the prehistoric origins of *M. leprae* can be retraced.

References and Notes

1. World Health Organization, *Wkly. Epidemiol. Rec.* **86**, 389 (2011).
2. S. T. Cole *et al.*, *Nature* **409**, 1007 (2001).
3. N. A. Groathouse *et al.*, *J. Clin. Microbiol.* **42**, 1666 (2004).
4. M. Monot *et al.*, *Science* **308**, 1040 (2005).
5. M. Monot *et al.*, *Nat. Genet.* **41**, 1282 (2009).
6. A. C. Stone, A. K. Wilbur, J. E. Buikstra, C. A. Roberts, *Am. J. Phys. Anthropol.* **140** (suppl. 49), 66 (2009).
7. C. Economou, A. Kjellström, K. Lidén, I. Panagopoulos, *J. Archaeol. Sci.* **40**, 465 (2013).
8. G. M. Taylor *et al.*, *J. Archaeol. Sci.* **36**, 2408 (2009).
9. K. I. Bos *et al.*, *Nature* **478**, 506 (2011).
10. J. L. Boldsen, *Am. J. Phys. Anthropol.* **135**, 301 (2008).
11. G. M. Taylor *et al.*, *PLoS ONE* **8**, e62406 (2013).
12. T. Maricic, M. Whitten, S. Pääbo, *PLoS ONE* **5**, e14004 (2010).
13. A. W. Briggs *et al.*, *Proc. Natl. Acad. Sci. U.S.A.* **104**, 14616 (2007).
14. V. J. Schuenemann *et al.*, *Proc. Natl. Acad. Sci. U.S.A.* **108**, E746 (2011).
15. S. Sawyer, J. Krause, K. Guschanski, V. Savolainen, S. Pääbo, *PLoS ONE* **7**, e34131 (2012).
16. A. Cooper, H. N. Poinar, D. N. A. Ancient, *Science* **289**, 1139b (2000).
17. M. Daffé, in *The Mycobacterial Cell Envelope*, M. Daffé, J.-M. Reyrat, Eds. (ASM Press, Washington, DC, 2008), pp. 3–11.
18. H. D. Donoghue *et al.*, *Lancet Infect. Dis.* **4**, 584 (2004).
19. T. Nguyen-Hieu, G. Aboudharam, M. Drancourt, *BMC Res. Notes* **5**, 528 (2012).
20. T. Lindahl, *Nature* **362**, 709 (1993).
21. S. Maeda *et al.*, *Antimicrob. Agents Chemother.* **45**, 3635 (2001).
22. R. W. Truman *et al.*, *N. Engl. J. Med.* **364**, 1626 (2011).
23. A. J. Drummond, A. Rambaut, *BMC Evol. Biol.* **7**, 214 (2007).
24. C. B. Ford *et al.*, *Nat. Genet.* **43**, 482 (2011).
25. G. Robbins *et al.*, *PLoS ONE* **4**, e5669 (2009).
26. B. E. Hart, R. I. Tapping, *J. Trop. Med.* **2012**, 1 (2012).
27. E. A. Misch, W. R. Berrington, J. C. Vary Jr., T. R. Hawn, *Microbiol. Mol. Biol. Rev.* **74**, 589 (2010).
28. M. E. Allentoft *et al.*, *Proc. Biol. Sci.* **279**, 4724 (2012).
29. T. Carver, N. Thomson, A. Bleasby, M. Berriman J. Parkhill, *Bioinformatics* **25**, 119 (2009).

Acknowledgments: We are grateful to the following people for providing samples, support, and advice: C. Bauer, H. Burbano, J. Hinds, S. Junker, M. Kodio, A. Fomba, C. Lanz, P. McLaren, J. Rougemont, and S. Schreiber. All raw read files have been deposited in the trace archive of the National Center for Biotechnology Information Sequence Read Archive under accession no. SRP022139. This work was supported by the European Research Council (ERC-APGREID), the Carl Zeiss Foundation, the Fondation Raoul Follereau, the Swiss National Science Foundation (Brazilian Swiss Joint Research Program), the Deutsche Forschungsgemeinschaft Priority Program 1335 Scalable Visual Analytics, the Central Innovation Program (grant KF2701103BZ1), the Graduate School Human Development in Landscapes, the Excellence Cluster Inflammation at Interfaces, the Medical Faculty of the Christian-Albrechts-University Kiel, a British Academy Small Research Grant, the Leverhulme Trust (Grant F/00094/BL), and the Social Sciences and Humanities Research Council of Canada (postdoctoral fellowship grant 756-2011-0501). Human remains were obtained under license from the UK Ministry of Justice.

Supplementary Materials

www.sciencemag.org/cgi/content/full/science.1238286/DC1
Materials and Methods
Figs. S1 to S9
Tables S1 to S14
References (*30*–*73*)

25 March 2013; accepted 28 May 2013
Published online 13 June 2013;
10.1126/science.1238286

Infectivity, Transmission, and Pathology of Human-Isolated H7N9 Influenza Virus in Ferrets and Pigs

H. Zhu,[1,2,3]* D. Wang,[8]* D. J. Kelvin,[4,5,6] L. Li,[1] Z. Zheng,[1] S.-W. Yoon,[7] S.-S. Wong,[7] A. Farooqui,[4] J. Wang,[1,3] D. Banner,[5] R. Chen,[1] R. Zheng,[1] J. Zhou,[1,2,3] Y. Zhang,[1] W. Hong,[1] W. Dong,[4] Q. Cai,[1] M. H. A. Roehrl,[5,6] S. S. H. Huang,[5,6] A. A. Kelvin,[4,5] T. Yao,[1] B. Zhou,[2] X. Chen,[2] G. M. Leung,[3] L. L. M. Poon,[2,3] R. G. Webster,[7] R. J. Webby,[7] J. S. M. Peiris,[2,3] Y. Guan,[1,2,3]† Y. Shu[8]†

The emergence of the H7N9 influenza virus in humans in Eastern China has raised concerns that a new influenza pandemic could occur. Here, we used a ferret model to evaluate the infectivity and transmissibility of A/Shanghai/2/2013 (SH2), a human H7N9 virus isolate. This virus replicated in the upper and lower respiratory tracts of the ferrets and was shed at high titers for 6 to 7 days, with ferrets showing relatively mild clinical signs. SH2 was efficiently transmitted between ferrets via direct contact, but less efficiently by airborne exposure. Pigs were productively infected by SH2 and shed virus for 6 days but were unable to transmit the virus to naïve pigs or ferrets. Under appropriate conditions, human-to-human transmission of the H7N9 virus may be possible.

On 31 March 2013, the Chinese National Health and Family Planning Commission announced the occurrence of three human infections with H7N9 subtype influenza viruses (*1*). Analyses of the sequences of the human H7N9 isolates indicate that the virus was derived by reassortment events between H7 and N9 subtype viruses, possibly from aquatic birds, and enzootic H9N2 viruses from chickens (*1*, *2*). As of 1 May 2013, more than 125 human cases have been confirmed, with the majority of the patients hospitalized and many suffering acute respiratory distress syndrome (*3*–*5*). More than 75% of human cases had a history of contact with, or exposure to, poultry before disease onset (*4*), suggesting a zoonotic origin of the infections. Identification of some family clusters raised concerns of human-to-human transmission by the H7N9 virus (*4*). Sequence analyses showed that the H7N9 viruses might have undergone mutations that are favorable for efficient replication in mammalian hosts (*2*, *6*–*8*).

To characterize this H7N9 virus, we assessed its infectivity, transmissibility, and pathogenicity in ferrets, the primary mammalian model for human influenza. Influenza-free ferrets ($n = 6$) were inoculated intranasally with 10^6 times the median tissue culture infectious dose ($TCID_{50}$) of A/Shanghai/02/2013 (SH2), a human isolate from a fatal index case (see supplementary materials and methods) (*1*). These ferrets displayed a brief fever at 1 to 2 days postinoculation (dpi) and robust sneezing and nasal discharge throughout the experiment (Table 1 and fig. S1, A, C, and D). Coughing and mild lethargy occurred

[1]Joint Influenza Research Centre [Shantou University Medical College (SUMC)/University of Hong Kong (HKU)], Shantou University, Shantou, PR China. [2]State Key Laboratory of Emerging Infectious Diseases (HKU-Shenzhen Branch), Shenzhen Third People's Hospital, Shenzhen, PR China. [3]State Key Laboratory of Emerging Infectious Diseases/Centre of Influenza Research, School of Public Health, The University of Hong Kong, Hong Kong SAR, PR China. [4]Joint Vaccine Research Centre [SUMC/University Health Network (UHN)], Shantou University Medical College, Shantou, PR China. [5]University Health Network, Toronto, Ontario, Canada. [6]University of Toronto, Toronto, Ontario, Canada. [7]Division of Virology, Department of Infectious Diseases, St. Jude Children's Research Hospital, Memphis, TN, USA. [8]National Institute for Viral Disease Control and Prevention, Chinese Center for Disease Control and Prevention, Key Laboratory for Medical Virology, National Health and Family Planning Commission, Beijing, PR China.

*These authors contributed equally to this work.
†Corresponding author. E-mail: yguan@hku.hk (Y.G.); yshu@cnic.org.cn (Y.S.)